2018

Development of Texture Weighted Fuzzy C-Means Algorithm for 3D Brain MRI Segmentation

Ji Young Lee
South Dakota State University

DEVELOPMENT OF TEXTURE WEIGHTED FUZZY C-MEANS ALGORITHM FOR 3D BRAIN MRI SEGMENTATION

BY

JI YOUNG LEE

A thesis submitted in partial fulfillment of the requirements for the

Master of Science

Major in Computer Science

South Dakota State University

2018

DEVELOPMENT OF TEXTURE WEIGHTED FUZZY C-MEANS ALGORITHM FOR 3D BRAIN MRI SEGMENTATION

JI YOUNG LEE

This thesis is approved as a creditable and independent investigation by a candidate for the Master of Science in Computer Science degree and is acceptable for meeting the thesis requirements for this degree. Acceptance of this does not imply that the conclusions reached by the candidate are necessarily the conclusions of the major department.

Sung Y. Shin, Ph.D.

Thesis Advisor Date

George Hamer, Ph.D.

Head, Department of Electrical Date

Engineering and Computer Science

Dean, Graduate School Date

This thesis is dedicated to my mentor, Denny.

ACKNOWLEDGEMENTS

I would like to say thank you to my advisor, Dr. Sung Shin for his considerable and continuous advice to me while I am doing my degree program. He gave me the valuable feedback not only for my research, but also on my way to be a researcher.

I also cannot say thank again to committee members of my thesis, Dr. Kwnaghee Won, Dr. Alireza Salehnia, and my graduate faculty representative, Dr. David Wiltse for their help to my thesis in the final defense. With their contributions, I could improve the quality of my thesis an even deeply and rationally. Also, I would like to thank CCT Lab members. I will never forget the day we studied together.

Finally, I do not have enough thanks to my family for their invaluable support that gave to me. Without their help, I could not continue my academic career.

TABLE OF CONTENTS

ABBREVIATIONS

CSF	cerebrospinal fluid
FCM	Fuzzy C-Means
GM	gray matter
INU	Intensity Non-Uniformity
LBP	Local Binary Pattern
LBP-TOP	Local Binary Patterns on Three Orthogonal Planes
MRI	Magnetic Resonance Image
TFCM	Texture weighted Fuzzy C-Means
VOI	Volume of Interest
WM	white matter

LIST OF FIGURES/TABLE

LIST OF EQUATIONS

ABSTRACT

DEVELOPMENT OF TEXTURE WEIGHTED FUZZY C-MEANS ALGORITHM FOR 3D BRAIN MRI SEGMENTATION

JI YOUNG LEE

2018

The segmentation of human brain Magnetic Resonance Image is an essential component in the computer-aided medical image processing research. Brain is one of the fields that are attracted to Magnetic Resonance Image segmentation because of its importance to human. Many algorithms have been developed over decades for brain Magnetic Resonance Image segmentation for diagnosing diseases, such as tumors, Alzheimer, and Schizophrenia. Fuzzy C-Means algorithm is one of the practical algorithms for brain Magnetic Resonance Image segmentation. However, Intensity Non-Uniformity problem in brain Magnetic Resonance Image is still challenging to existing Fuzzy C-Means algorithm.

In this paper, we propose the Texture weighted Fuzzy C-Means algorithm performed with Local Binary Patterns on Three Orthogonal Planes. By incorporating texture constraints, Texture weighted Fuzzy C-Means could take into account more global image information. The proposed algorithm is divided into following stages: Volume of Interest is extracted by 3D skull stripping in the pre-processing stage. The initial Fuzzy C-Means clustering and Local Binary Patterns on Three Orthogonal Planes feature extraction are performed to extract and classify each cluster's features. At the last stage, Fuzzy C-Means with texture constraints refines the result of initial Fuzzy C-Means.

The proposed algorithm has been implemented to evaluate the performance of segmentation result with Dice's coefficient and Tanimoto coefficient compared with the ground truth. The results show that the proposed algorithm has the better segmentation accuracy than existing Fuzzy C-Means models for brain Magnetic Resonance Image.

INTRODUCTION

Magnetic Resonance Imaging is one of the most popular non-invasive imaging techniques for human brain [1]. Segmentation of brain Magnetic Resonance Image (MRI) is useful for clinical purposes according to the characteristics of each part [1-6]. The segmentation has been performed for three types of tissues: cerebrospinal fluid (CSF), gray matter (GM), and white matter (WM). The segmented MRI helps medical experts in diagnosing various diseases such as tumors, Alzheimer, and Schizophrenia [7].

Various segmentation methods have been suggested for brain MRI segmentation due to its complicated structure and absence of a well-defined boundary between different tissues [8] such as edge detection [10], region growing [11], classification method [12], and clustering method [1][9]. Fuzzy C-Means (FCM) clustering is one of the most popular clustering methods because of its robust characteristics for segmentation [9,13]. It assigns each pixel to one of the pre-defined classes according to the similarities to the clusters. Ahmed *et al.* [15] and many researchers introduced various spatial FCM methods that consider not only the pixel itself but also its neighboring pixels [15,17-21]. However, spatial FCM methods still suffer from Intensity Non-Uniformity (INU) problem in brain MRI because FCM easily falls into local minima [22]. In this paper, we propose the Texture weighted Fuzzy C-Means (TFCM) which considers not only intensities of local neighbors but also texture patterns of them. It makes use of Local Binary Patterns on Three Orthogonal Planes (LBP-TOP) feature to represent texture information of each pixel and neighboring region and embed the information into the objective function of FCM.

The rest of this paper is organized as follows: BACKGROUND section briefly introduces fundamental of related algorithms; RELATED WORK section briefly reviews related methodologies and applications; MATERIAL AND METHODS section describes the proposed algorithm; RESULT AND ANALYSIS presents the evaluated results; CONCLUSION shows the conclusions.

BACKGROUND

Fuzzy C-Means Clustering Algorithm

Clustering is an unsupervised technique which analyzes and finds the hidden patterns from the raw and unlabeled data. Clustering partitions the data into groups (or clusters) based on some measurements for similarities and shared characteristics among the data. So, the data in the same clusters have similar characteristics after clustering, while the data in the different clusters have rare characteristics.

FCM clustering algorithm is developed by Dunn [37]. In image processing, FCM assigns each pixel (or voxel) to one of the pre-defined classes according to the similarities to the clusters. Different from K-Means clustering algorithm, one of the most famous clustering algorithms, FCM allows one piece of data to belong to two or more clusters which is called the soft clustering, while K-Means allows the data to belong to only one clusters which is called the hard clustering.

FCM aim to minimize the objective function which is called cost function in machine learning. The objective function of FCM is consist of two parts, membership function and similarity between measured data and center of the cluster.

$$J_m = \sum_{j=1}^{N} \sum_{i=1}^{C} u_{ij}^{m} d^2(x_j, v_i) \quad (1)$$

where N indicates the number of pixels in the whole image, C indicates the number of clusters, u_{ij} represents the membership function of the *j*th pixel to respect cluster *i*, *m*

indicates the fuzzification factor that controls the effect of fuzziness, and $d^2(.)$ represents the Euclidian distance between the measured data x_j and the cluster center v_i.

The membership function u_{ij} refers to the probability that each pixel (or voxel) is belongs to each cluster. The range of the membership function is 0 to 1. Thus, u_{ij} satisfy the constraints $\sum_{i=1}^{C} u_{ij} = 1$ for $\forall j\ 1 \leq j \leq N$. To minimize the objective function, taking the derivative of Equation 1 respect to membership function u_{ij}. Then, u_{ij} is obtained as

$$u_{ij} = \frac{1}{\sum_{k=1}^{C} \left(\frac{d(x_j, v_i)}{d(x_j, v_k)} \right)^{2/(m-1)}} \tag{2}$$

Euclidian distance is typically used to represent the similarity between measured data and center of the cluster as Equation 3.

$$d^2(x_j, v_i) = \left\| x_j - v_i \right\|^2 \tag{3}$$

Figure 1 shows the updating progress of membership function during the FCM iteration with Iris flower dataset provided from MATLAB library [38]. This is a multivariate dataset which consists of 150 observations with 3 species; Iris setosa, Iris virginica, and Iris versicolor with 4 features; sepal length, sepal width, petal length, and petal width. The graph plotted the membership function of the data for each cluster 1 to 3 with different colors. Figure 1 (a) shows the randomly initialized membership function. Through Figure 1 (b) to (c), membership functions of the data are being gradually rearranged to the end.

a)

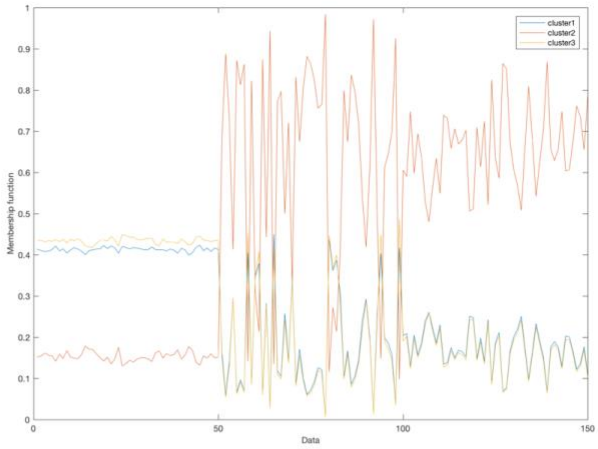

b)

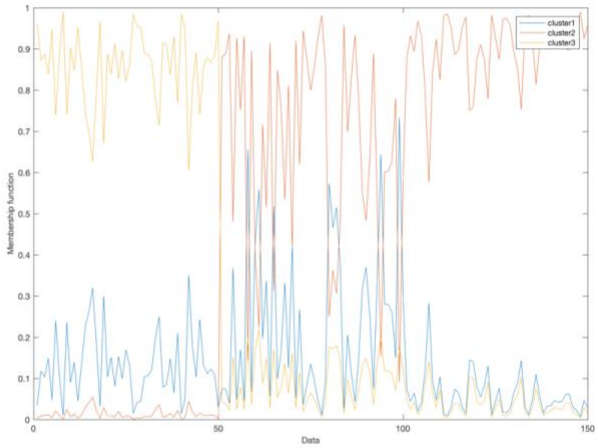

c)

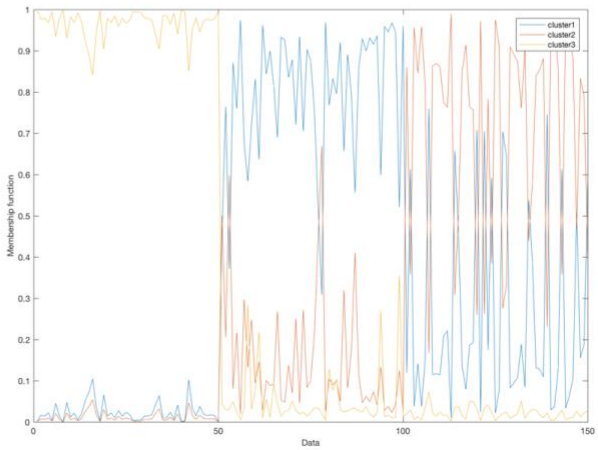

Figure 1. Membership function of FCM with Iris dataset. a) iteration = 1, b) iteration = 6, and c) iteration = 32.

For example, the membership function of data 1 at 1st iteration is

$$X = \begin{bmatrix} 0.4138 & 0.1519 & 0.4344 \\ \vdots & \vdots & \vdots \end{bmatrix}$$

At 6th iteration, the membership function of data 1 is

$$X = \begin{bmatrix} 0.0349 & 0.0030 & 0.9621 \\ \vdots & \vdots & \vdots \end{bmatrix}$$

At 32nd iteration, the membership function of data 1 is

$$X = \begin{bmatrix} 0.0023 & 0.0011 & 0.9966 \\ \vdots & \vdots & \vdots \end{bmatrix}$$

The data 1 is clustered to 3rd cluster, since the highest membership value for each cluster of data 1 is 0.9966 for 3rd cluster.

Similar to membership function, taking the derivative of Equation 1 respect to cluster center v_i, then we obtained

$$v_i = \frac{\sum_{j=1}^{N} (u_{ij})^m x_j}{\sum_{j=1}^{N} (u_{ij})^m} \tag{4}$$

Equation 2 and 4 are the two necessary conditions for J_m to be at its local optimization. Every iteration, FCM update the membership function and the cluster center based on Equation 2 and 4, respectively, and calculate the new objective function based on Equation 1 to aim to minimize it.

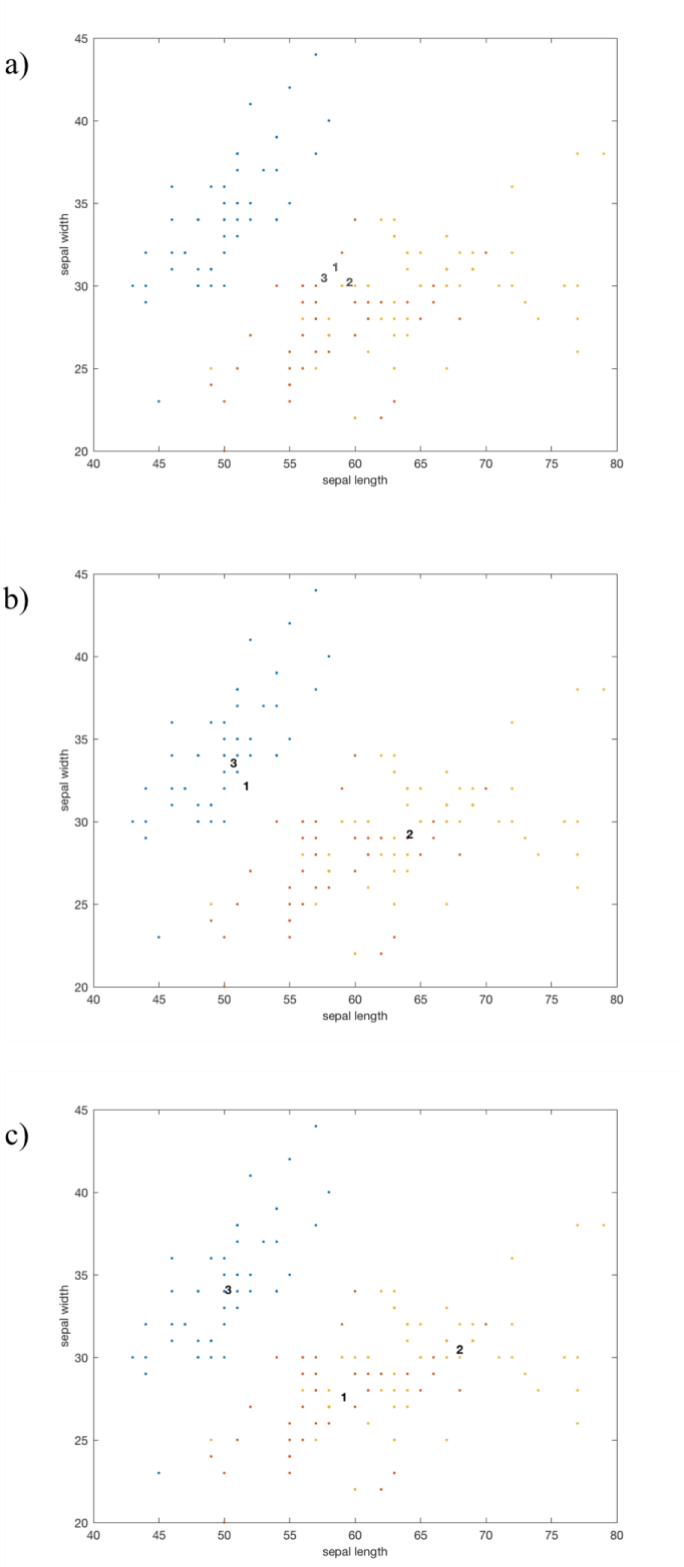

Figure 2. Cluster center of FCM with Iris dataset. a) iteration = 1, b) iteration = 6, and c) iteration = 32.

Figure 2 shows the updating progress of cluster center during the FCM iteration with Iris flower dataset. The graph scattered the data based on sepal length and sepal width in centimeters unit. The bold number from 1 to 3 indicates the cluster center of each 1st to 3rd cluster. Figure 2 (a) shows the randomly initialized cluster centers. Through Figure 2 (b) to (c), we can visually notice that cluster centers are being gradually relocated to the end.

Local Binary Pattern Feature Extraction Operator

Ojala *et al*. [27,28] introduced Local Binary Pattern (LBP), which is a very simple and efficient discriminative texture descriptor to extract texture patterns from the image [29]. The LBP operator in [28] was defined as

$$LBP = \sum_{p=0}^{P-1} sign(v_p - v_c)2^P \tag{5}$$

$$sign(x) = \begin{cases} 0, & x < 0 \\ 1, & x \geq 0 \end{cases}$$

where P is the total number of neighboring pixels, v_c and v_p are the intensity values of the center pixel and its neighborhood pixels respectively.

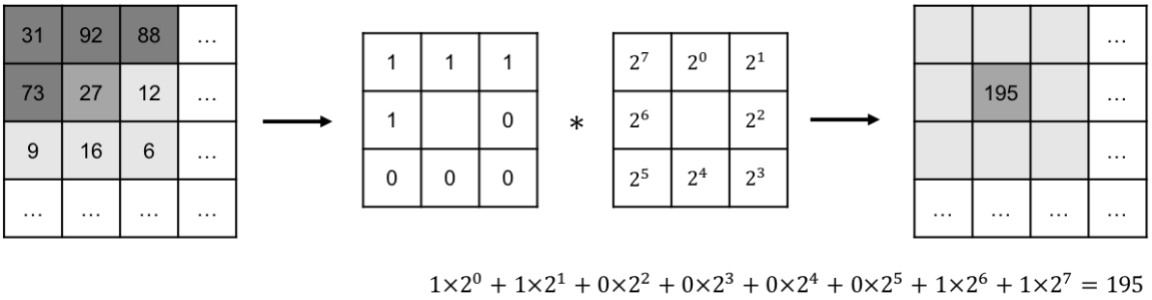

Figure 3. Encoding process of LBP operator.

Figure 3 shows the example of how LBP value is encoded. Pixel with 27 intensity value threshold neighbor pixels within 3x3 window and multiply power of 2 matrix. The final encoding LBP value is 195. The LBP value is used as a bin of histogram that count the number of pixels who have the LBP value.

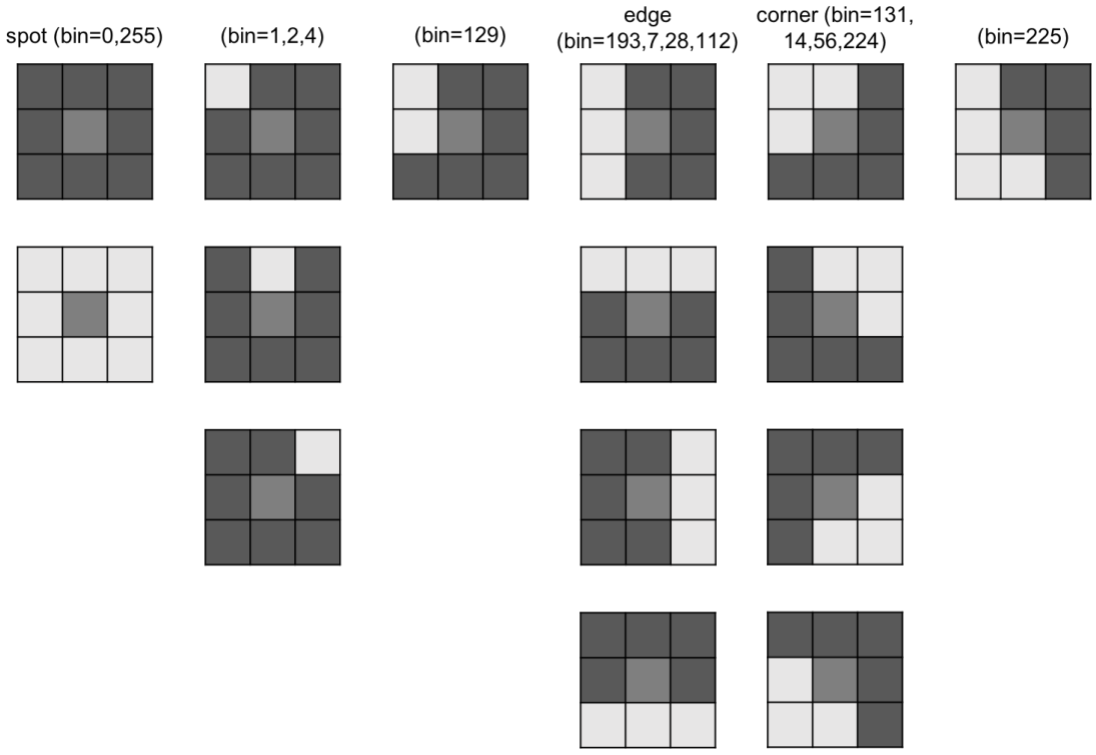

Figure 4. Examples of 2D encoded patterns by histogram bins when $P = 8$.

Each unique LBP value is used as a minimal unit of texture representation and refers to the value of the x-axis of the histogram. Figure 4 shows the labeled pixels with computed LBP value. For example, LBP value (or bin number of histogram) 193, 7, 28, or 112 indicates edges. These computed LBP values would be used as a texture descriptor for the pixels (or voxels) within the image.

RELATED WORK

FCM is a soft clustering method based on fuzzy set theory [1,9,14,16]. It performs similar with K-Means algorithm but allows each pixel to belong to multiple classes according to a certain membership value [1]. Local minima is one of the well-known drawbacks of FCM method [22]. To deal with the problem, various spatial FCM methods have been proposed.

Ahmed *et al.* [15] introduced the first spatial FCM method FCM_S by modifying the objective function to compensate intensity inhomogeneity. In this method, each pixel in a whole image was labeled with considering its immediate neighborhood. However, FCM_S is sensitive to noise and time-consuming. Chen *et al.* [17] proposed FCM_S1 and FCM_S2 based on FCM_S by applying mean filter and median filter in advance respectively. They also simplified the neighborhood term of the objective function of FCM_S. FCM_S1 and FCM_S2 improved the immunity to Gaussian noise and impulse noise. However, they are still weak to salt and pepper noise. Szilágyi *et al.* [18] proposed EnFCM with the reconstructed image prior to segmentation. Linear weighted sum method performed clustering the image based on the gray-level histogram instead of pixels in an image. Time complexity was greatly reduced with this algorithm, but it requires prior knowledge for choosing major parameters and only works on gray-level images. Cai *et al.* [19] proposed FGFCM by incorporating local spatial and gray information. They enhanced the flexibility to select the spatial term control parameter, but still dependent on another parameter selection. Krinidis *et al.* [20] proposed FLICM with a new fuzzy factor, which does not require pre-processing. It is a parameter

determination free algorithm, but FLICM is time-consuming for large-scale image since it requires several iteration steps on the same window. With previous work, we proposed TFCM algorithm. The proposed algorithm suggested a global and accurate model by incorporating texture terms to intensity distance.

MATERIAL AND METHODS

In this section, our proposed algorithm and its preliminary are introduced. Figure 5 shows the overview of the proposed algorithm. The algorithm firstly pre-processes the original image for Volume of Interest (VOI) extraction using 3D Skull Stripping. Then, the feature extraction and classification are performed using LBP-TOP and initial FCM. The classified texture information of each White Matter, Gray Matter, and Cerebrospinal Fluid cluster are used as texture constraints of final TFCM segmentation algortihm.

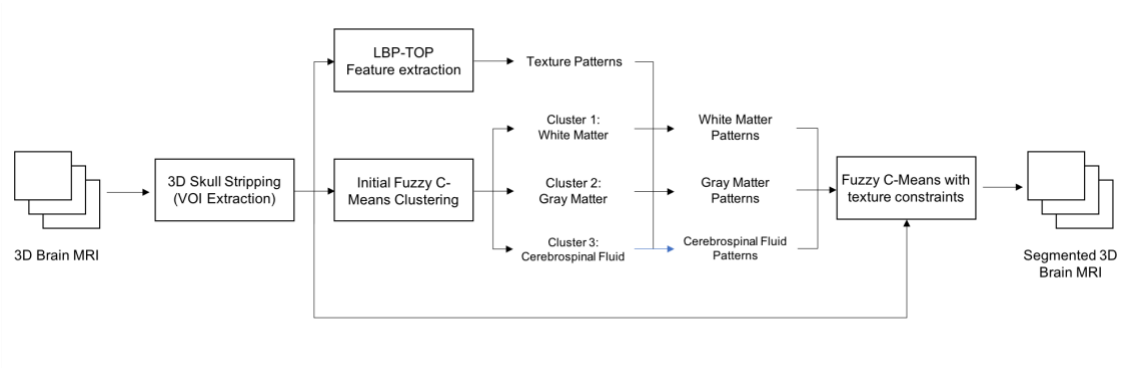

Figure 5. Overview of the methodology.

3D Skull Stripping

In order to reduce the effect of background noise and time complexity, extra-cranial tissues were removed from the input image before segmentation. To extract the VOI region, several pre-processing techniques such as thresholding, morphological operation [24], and skull stripping algorithm were performed. In this paper, we used

3DSkullStrip by Smith *et al.* [23,25,26] as a skull stripping method to extract the VOI region.

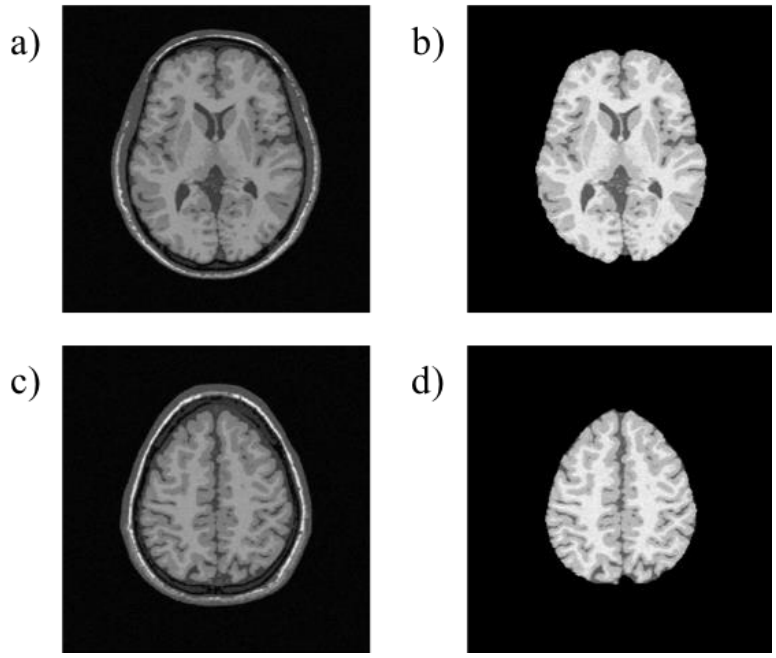

Figure 6. VOI extraction using 3D Skull Stripping: (a), (c) Original image. (b), (d) VOI extracted image.

Initial Fuzzy C-Means

The conventional Fuzzy C-Means algorithm was performed to classify the features from each type of tissue such as WM, GM, CSF, and background. Segmentation refinement was performed with the proposed algorithm introduced in following sections after extracting classified features.

Feature Extraction

Zhao *et al*. [30] proposed LBP for spatiotemporal data by concatenating LBP on three orthogonal planes, i.e., the xy-, xt-, and yt-planes. We applied LBP-TOP to brain volume image as in [23], we also used z-dimension instead of t-dimension. In the proposed algorithm, a histogram of each plane was summed up rather than concatenated to exaggerate the distribution of the encoding values. The modified histogram could obtain more distinct features since brain volume image has similar texture patterns in xy-, xz-, and yz-planes.

The LBP operator in (5) could not distinguish each tissue since the key factor to classify the brain volume is the intensity values. The proposed algorithm modified LBP-TOP by incorporating texture patterns and intensity values to specify the estimating intensity range of tissues. The equation (5) is modified as

$$LBP = \sum_{p=0}^{P-1} sign(v_p - v_c)2^P L_c \qquad (6)$$

$$sign(x) = \begin{cases} 0, & x < 0 \\ 1, & x \geq 0 \end{cases}$$

where L_c denotes the initially extracted class index by Fuzzy C-Means. Figure 6 shows the derived normalized histogram of each cluster after feature classification. The x-axis of the histogram represents the LBP value obtained from (6), and the y-axis represents the probability of occurrence. The extracted features are classified into 4 clusters by using

initial FCM as described in previous section. The normalized encoding value is used as a texture membership probability of each voxel to each cluster.

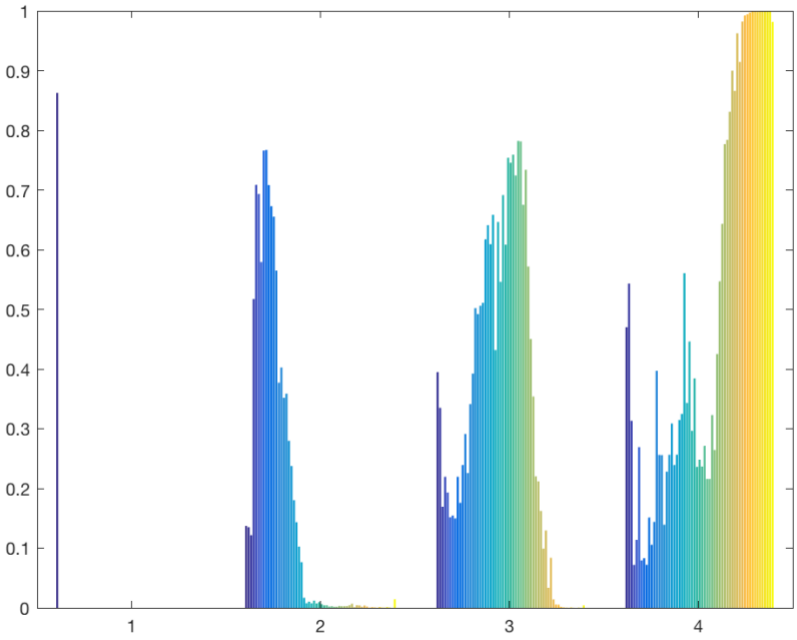

Figure 6. Extracted LBP-TOP histogram of each tissue: 1 is background, 2 is cerebrospinal fluid, 3 is gray matter, and 4 is white matter.

3D Fuzzy C-Means with Texture Constraints

Preliminaries

Various Fuzzy C-Means improved invariants algorithms have been developed by many researchers as we researched in related work section. Many researchers have studied to enhance the models' performance in 2 ways: Segmentation accuracy and speed. The very first model of modification to the conventional FCM to improve the segmentation accuracy was proposed by Ahmed et al. [15] which is called FCM_S by introducing neighbor term to the original objective function. The introduced neighbor term allows the influence of its immediate neighboring pixels when labeling the pixel. This term regularizes the intensities within the neighborhood window so that can get the piecewise homogeneous labeling solution. The objective function of conventional FCM (1) is modified as

$$J_m = \sum_{i=1}^{c}\sum_{k=1}^{N} u_{ik}^{\mathrm{m}}\|x_k - v_i\|^2 + \frac{\alpha}{N_R}\sum_{i=1}^{c}\sum_{k=1}^{N} u_{ik}^{\mathrm{m}} \sum_{r\in N_k}\|x_r - v_i\|^2 \qquad (7)$$

where c is the number of cluster, N is the number of pixels in image, x_k is the intensity value of the *k*th pixel, v_i represents the center value of the *i*th cluster, u_{ik} represents the fuzzy membership of the *k*th pixel to respect cluster i, N_R is its cardinality, x_r represents the neighbor of x_k, and N_k represents the set of neighbor within a window around x_k. The parameter m is a weighting exponent on each fuzzy membership that determines the

amount of fuzziness of the resulting classification. The parameter α is used to control the effect of the neighbor term.

By the definition, each sample point x_k satisfies the constraint that $\sum_{i=1}^{c} u_{ik} = 1$. Two necessary conditions for J_m to be at its local optimization will be obtained as

$$u_{ik} = \frac{\left(\|x_k - v_i\|^2 + \frac{\alpha}{N_R}\sum_{r\in N_k}\|x_r - v_i\|^2\right)^{-1/(m-1)}}{\sum_{j=1}^{c}\left(\|x_k - v_j\|^2 + \frac{\alpha}{N_R}\sum_{r\in N_k}\|x_r - v_j\|^2\right)^{-1/(m-1)}} \tag{8}$$

$$v_i = \frac{\sum_{k=1}^{N} u_{ik}^m (x_k + \frac{\alpha}{N_R}\sum_{r\in N_k} x_r)}{(1+\alpha)\sum_{k=1}^{N} u_{ik}^m} \tag{9}$$

But there was a trade-off that FCM_S improved the segmentation accuracy compared to conventional FCM model but resulted with the high computational cost since every pixel has to compute the neighborhood influence when labeling the pixel.

Szilágyi *et al.* [18] proposed a modified spatial FCM algorithm EnFCM by speeding up the segmentation process for the gray-level image. In order to accelerate the time performance of previous spatial FCM methods, a linearly-weighted sum image is formed in advance from the original image. The local neighbor average image is obtained in terms of

$$\xi_k = \frac{1}{1+\alpha}(x_k + \frac{\alpha}{N_R}\sum_{j\in N_k} x_j) \tag{10}$$

where ξ_k denotes the gray value of the *k*th pixel of image ξ, x_k is the intensity value of the *k*th pixel, N_R is the cardinality, N_k represents the set of neighbors within a window around x_k, and x_j represents the neighbors of x_k. The parameter α is used to control the effect of the neighbor term. EnFCM is performed on the gray-level histogram of the generated image ξ. The objective function of the EnFCM is defined as

$$J_s = \sum_{i=1}^{c} \sum_{l=1}^{q} \gamma_l u_{il}^m (\xi_l - v_i)^2 \tag{11}$$

where u_{il} represents the fuzzy membership of gray value l with respect to cluster *i* and v_i represents the center value of the *i*th cluster. The parameter m is a weighting exponent on each fuzzy membership that determines the amount of fuzziness of the resulting classification. c denotes the total number of cluster and q denotes the number of the gray-levels of the given image, and *N* is the number of pixels in an image. γ_l is the number of the pixels having the gray value equal to *l* where $l = 1, \dots, q$. So, one of the constraints of *l* is defined as

$$\sum_{l=1}^{q} \gamma_l = N \tag{12}$$

By the definition, each pixel x_k satisfies the constraint that $\sum_{i=1}^{c} u_{ik} = 1$ for any *l*. Two necessary conditions for J_s to be at its local optimization will be obtained as

$$u_{il} = \frac{(\xi_l - v_i)^{-2/(m-1)}}{\sum_{j=1}^{c} (\xi_l - v_j)^{-2/(m-1)}} \tag{13}$$

$$v_i = \frac{\sum_{l=1}^{q} \gamma_l u_{il}^m \xi_l}{\sum_{l=1}^{q} \gamma_l u_{il}^m} \tag{14}$$

Texture weighted Fuzzy C-Means

We designed the clustering process of TFCM with extracted texture in (6) as t_{ik} for *k*th voxel to cluster i. The texture membership probability t_{ik} for all *k* is computed in advance as described in previous section. Initially, we designed the TFCM based on FCM_S on the purpose of improving the accuracy. The objective function is modified as

$$J_{t1} = \sum_{i=1}^{c}\sum_{k=1}^{N} u_{ik}^{\mathrm{m}} \|x_k - v_i\|^2 + \alpha \sum_{i=1}^{c}\sum_{k=1}^{N} (\beta u_{ik} + (1-\beta) t_{ik})^m \|\overline{x_k} - v_i\|^2 \tag{15}$$

where t_{ik} represents the texture membership of the *k*th voxel to *i*th cluster, parameter β controls the effect of the intensity features and texture features.

The constrained optimization will be solved using one Lagrange multiplier as

$$\begin{aligned} F_m = &\sum_{i=1}^{c}\sum_{k=1}^{N} (u_{ik}^{\mathrm{m}} \|x_k - v_i\|^2 + \alpha(\beta u_{ik} + (1-\beta) t_{ik})^m \|\overline{x_k} - v_i\|^2) \\ &+\lambda(1 - \sum_{j=1}^{c} (\beta u_{ij} + (1-\beta) t_{ij})) \end{aligned} \tag{16}$$

Taking the derivative of F_m with respect to u_{ik} and setting the result to zero, we have, for $m > 1$

$$\frac{dF_m}{du_{ik}} = \left(\frac{\beta\lambda}{m\|x_k - v_i\|^2 + \alpha\beta\|\overline{x_k} - v_i\|^2}\right)^{1/(m-1)} \tag{17}$$

By constraints $\sum_{i=1}^{c} u_{ik} = 1$ for all *k*, we obtained

$$\lambda = \frac{m}{\beta\left(\sum_{j=1}^{c}(\|x_k - v_i\|^2 + \alpha\beta\|\overline{x_k} - v_i\|^2)^{-\frac{1}{m-1}}\right)^{m-1}} \tag{18}$$

Substituting into equation #, the zero-gradient condition for the membership function can be written as

$$u_{ik} = \frac{(\|x_k - v_i\|^2 + \alpha\beta\|\overline{x_k} - v_i\|^2)^{-1/(m-1)}}{\sum_{j=1}^{c}\left(\|x_k - v_j\|^2 + \alpha\beta\|\overline{x_k} - v_j\|^2\right)^{-1/(m-1)}} \tag{19}$$

Similarly, cluster center is obtained as

$$v_i = \frac{\sum_{k=1}^{N}(u_{ik}^m(x_k + \alpha\beta\overline{x_k})) + \alpha(1-\beta)t_{ik}^m\overline{x_k}}{\sum_{k=1}^{N}\left((1+\alpha\beta)u_{ik}^m + \alpha(1-\beta)t_{ik}^m\right)} \tag{20}$$

But the time complexity of the proposed algorithm was too high, so we redesigned the objective function based on EnFCM. The revised objective function is defined as

$$J_t = \sum_{i=1}^{c}\sum_{l=1}^{q} \gamma_l(\beta u_{il} + (1-\beta)t_{il})^m(\xi_l - v_i)^2 \tag{21}$$

Similar with (15), t_{ik} represents the texture membership of the *k*th voxel to *i*th cluster. The parameter β controls the effect of the intensity distance features and texture features. The constrained optimization was solved using one Lagrange multiplier as

$$\begin{aligned} F_t = \sum_{i=1}^{c}\sum_{l=1}^{q} [\gamma_l(\beta u_{il} + (1-\beta)t_{il})^m(\xi_l - v_i)^2] \\ + \sum_{l=1}^{q} \lambda_l \left(1 - \sum_{i=1}^{c}(\beta u_{il} + (1-\beta)t_{il})\right) \end{aligned} \tag{22}$$

Taking the derivative of F_t with respect to u_{il} and setting the result to zero for $m > 1$, we have

$$\frac{dF_t}{du_{il}} = m\beta\gamma_l(\xi_l - v_i)^2(\beta u_{il} + (1-\beta)t_{il})^{m-1} - \beta\lambda_l = 0 \tag{23}$$

For u_{il}, we obtained

$$u_{il} = \frac{1}{\beta}\left[\left(\frac{\lambda_l}{m\gamma_l(\xi_l - v_i)^2}\right)^{1/(m-1)} - (1-\beta)t_{il}\right] \tag{24}$$

By constraints $\sum_{i=1}^{c}[\beta u_{il} + (1-\beta)t_{il}] = 1$ for all $l > 0$, we obtained

$$\lambda_l = \left(\sum_{j=1}^{c} \left(m\gamma_l \left(\xi_l - v_j \right)^2 \right)^{1/(m-1)} \right)^{m-1} \tag{25}$$

Substituting into (24), the zero-gradient condition for the u_{il} can be written as

$$u_{il} = \frac{1}{\beta} \sum_{j=1}^{c} \left(\frac{\xi_l - v_j}{\xi_l - v_i} \right)^{2/(m-1)} - \frac{1-\beta}{\beta} t_{il} \tag{26}$$

Similarly, taking the derivative of F_t with respect to v_i, we have

$$\frac{dF_t}{dv_i} = -2 \sum_{l=1}^{q} \gamma_l (\beta u_{il} + (1-\beta) t_{il})^m (\xi_l - v_i) = 0 \tag{27}$$

Then, the cluster center is defined as

$$v_i = \frac{\sum_{l=1}^{q} \gamma_l (\beta u_{il} + (1-\beta) t_{il})^m \xi_l}{\sum_{l=1}^{q} \gamma_l (\beta u_{il} + (1-\beta) t_{il})^m} \tag{28}$$

Through the iteration, TFCM aim to minimize the its objective function (21) by revising the membership functions and cluster centers with pre-defined texture and intensity information of each voxel based on (26) and (28), respectively.

The pseudo code of the proposed TFCM algorithm is as follows:

Algorithm 1 TFCM

Step 1:	Set the cluster number *c*, maximum iteration number I, error rate ε, fuzziness parameter *m*, cardinality N_R, and the term control parameter α and β.
Step 2:	Extract features of each cluster from an original image and set t.
Step 3:	Classify the extracted features into *c* clusters.
Step 4:	Form the new local neighbor average image ξ (10) and its histogram.
Step 5:	Randomly initialize the fuzzy membership matrix as U^0 (26) and objective function matrix as J_t^0 (21).
Step 6:	Set the loop counter i to zero.
Step 7:	Update the cluster centers (28).
Step 8:	Update the fuzzy membership matrix U^{i+1} at counter i (26).
Step 9:	Update the objective function J_t^{i+1} at counter i (21).
Step 10:	If $J_t^{i+1} - J_t^{ii} < \varepsilon$ or loop counter met *I* then stop, otherwise set $i = i + 1$ and then go to Step 7.

RESULT AND ANALYSIS

In this section, the proposed algorithm was applied to 20 anatomical models of normal brain MR image volumes provided by the BrainWeb database with ground truths [31-33]. The provided dataset is a set of T1-weighted simulated data with these specific parameters: SFLASH (spoiled FLASH) sequence with TR (repetition time)=22ms, TE (echo time)=9.2ms, flip angle=30 degree and 1 mm isotropic voxel size with a resolution of 256×256×181 per volume [34,35].

The number of clusters was set as 4 – background, CSF, GM, and WM. The number of maximum iteration number was set as 100, error threshold as 1×10^{-5}, fuzziness parameter as 2, and parameter α was set to 4.2 as same as previous methods. For 3D window, the cardinality was set to 6: $\pm$1-pixel volume distance in each x-, y-, and z-axis. The texture and intensity constraints control parameter β was set to 0.8 which was found empirically. Figure 7 shows the 2D sliced images for the VOI extracted and segmented image volume.

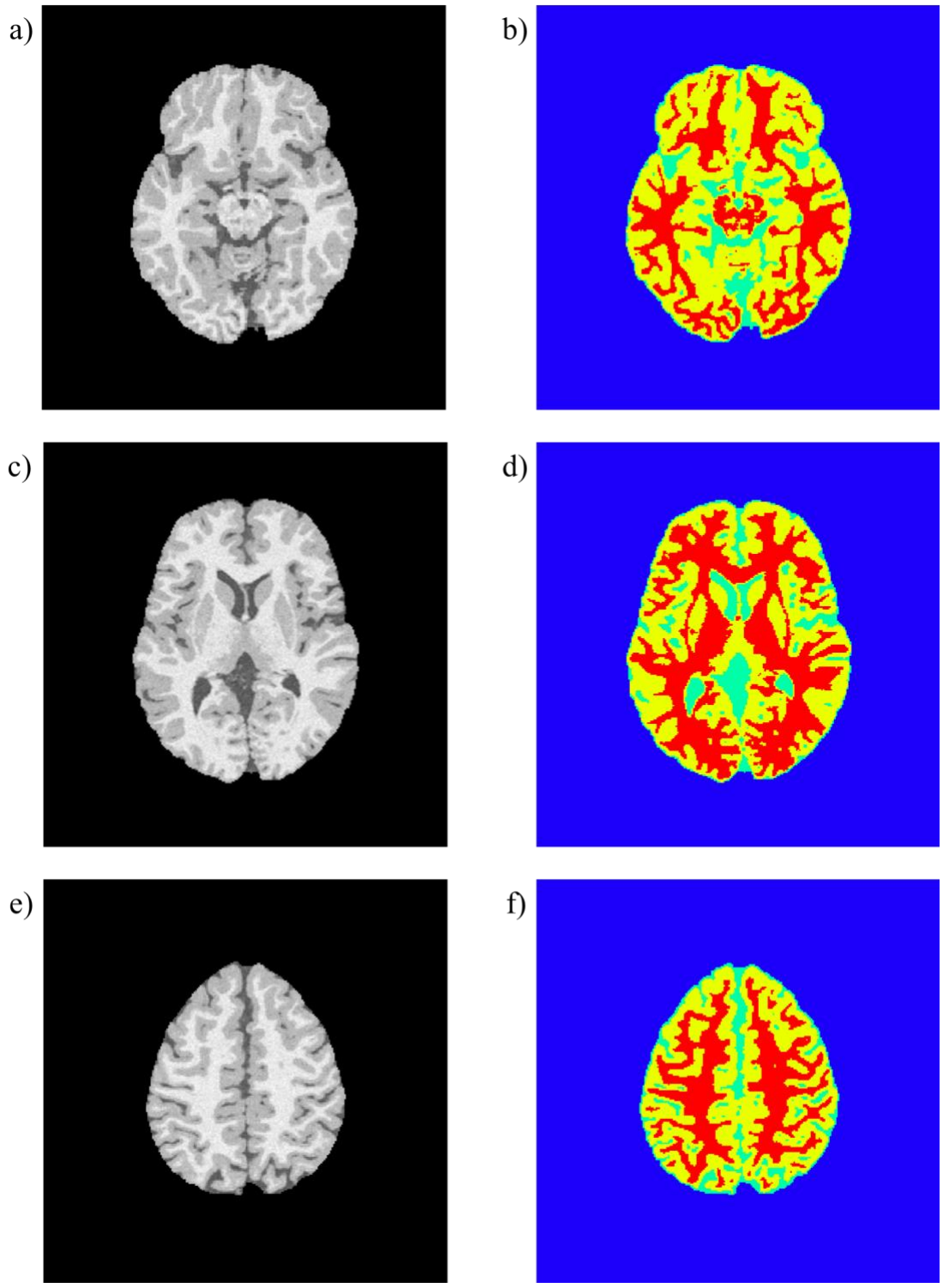

Figure 7. T1-weighted normal brain MRI from BrainWeb database: (a), (c), and (e) VOI extracted original Image. (b), (d), and (f) segmented Image.

To quantitatively evaluate the performance of TFCM, Dice's Coefficient (DC) [36] and Tanimoto Coefficient (TC) [7] were used and compared with several FCM applicants. We have programmed the operation results of the models other than the model of [7], and the operation results of the [7] are referred to the author 's paper.

The DC and TC are defined by

$$DC(MS, GT) = \frac{2|MS \cap GT|}{|MS| + |GT|} \tag{16}$$

$$TC(MS, GT) = \frac{|MS \cap GT|}{|MS \cup GT|} \tag{17}$$

where $|.|$ denotes the number of pixels included in the region, *MS* and *GT* are the regions segmented by the method and by the ground truth, respectively. Both DC and TC metrics indicates higher segmentation accuracy when the value reaches 1. Our model was written with the image processing library in MATLAB, tested on 2.8GHz Intel Core i7 with 16GB 2133 MHz LPDDR3 memory, and compared with published Fuzzy C-Means methods on brain MRI segmentation.

Table 1. Comparison of DC and TC for BrainWeb dataset.

Methods	DC	TC
FCM [14]	0.7230	0.6142
FCM_S [15]	0.7823	0.6142
FCM_S1 [17]	0.8909	0.7882
FCM_S2 [17]	0.9327	0.8743
EnFCM [18]	0.9152	0.8235

FGFCM [19]	0.9243	0.8620
FLICM [20]	0.9021	0.7781
BCSFCM [7]	0.9504	0.8872
TFCM	**0.9543**	**0.9322**

Table 1 shows the evaluated performance of TFCM and other algorithms. The results show the proposed algorithm has a noticeable improvement in TC with the well-classified intersection between segmented model and ground truth. These results suggest that the proposed algorithm is highly accurate in TC even though there was not a significant improvement in DC. We would continue this study to improve the segmentation accuracy for both coefficients in the near future.

CONCLUSION

Accurate brain MRI segmentation is the important components for its clinical purpose [1-8]. In this paper, texture weighted TFCM method is proposed. The experimental result shows that TFCM is meaningful to segment brain structures by reducing the effect of INU from the brain MRI by incorporating texture constraints with intensity feature distances. With this result, the proposed algorithm shows the feasibility to be used for clinical evaluation of diseases in the brain such as brain tumors, Alzheimer, and Schizophrenia. We tested and evaluated the result with normal brain datasets in this paper, but we would like to expand our study with the lesion brain datasets for future.

LITERATURE CITED

1. Despotović, I., Goossens, B., & Philips, W. (2015). MRI segmentation of the human brain: challenges, methods, and applications. *Computational and mathematical methods in medicine, 2015*.
2. Bauer, S., Wiest, R., Nolte, L. P., & Reyes, M. (2013). A survey of MRI-based medical image analysis for brain tumor studies. *Physics in Medicine & Biology*, *58*(13), R97.
3. Wen, P. Y., Macdonald, D. R., Reardon, D. A., Cloughesy, T. F., Sorensen, A. G., Galanis, E., ... & Tsien, C. (2010). Updated response assessment criteria for high-grade gliomas: response assessment in neuro-oncology working group. *Journal of clinical oncology*, *28*(11), 1963-1972.
4. Black, P. M. (1991). Brain tumors. *New England Journal of Medicine*, *324*(22), 1555-1564.
5. Balafar, M. A., Ramli, A. R., Saripan, M. I., & Mashohor, S. (2010). Review of brain MRI image segmentation methods. *Artificial Intelligence Review*, *33*(3), 261-274.
6. Han, X., & Fischl, B. (2007). Atlas renormalization for improved brain MR image segmentation across scanner platforms. *IEEE transactions on medical imaging*, *26*(4), 479-486.
7. Prakash, R. M., & Kumari, R. S. S. (2017). Spatial fuzzy C means and expectation maximization algorithms with bias correction for segmentation of mr brain images. *Journal of medical systems*, *41*(1), 15.

8. Verma, H., Agrawal, R. K., & Sharan, A. (2016). An improved intuitionistic fuzzy c-means clustering algorithm incorporating local information for brain image segmentation. *Applied Soft Computing*, *46*, 543-557.
9. Naz, S., Majeed, H., & Irshad, H. (2010, October). Image segmentation using fuzzy clustering: A survey. In *Emerging Technologies (ICET), 2010 6th International Conference on* (pp. 181-186). IEEE.
10. Batista, J., & Freitas, R. (1999). An adaptive gradient-based boundary detector for MRI images of the brain.
11. Fan, J., Yau, D. K., Elmagarmid, A. K., & Aref, W. G. (2001). Automatic image segmentation by integrating color-edge extraction and seeded region growing. *IEEE transactions on image processing*, *10*(10), 1454-1466.
12. Duda, R. O., Hart, P. E., & Stork, D. G. (1973). *Pattern classification* (Vol. 2). New York: Wiley.
13. Ortiz, A., Palacio, A. A., Górriz, J. M., Ramírez, J., & Salas-González, D. (2013). Segmentation of brain MRI using SOM-FCM-based method and 3D statistical descriptors. *Computational and mathematical methods in medicine*, *2013*.
14. Bezdek, J. C. (1981). Objective Function Clustering. In *Pattern recognition with fuzzy objective function algorithms* (pp. 43-93). Springer, Boston, MA.
15. Ahmed, M. N., Yamany, S. M., Mohamed, N., Farag, A. A., & Moriarty, T. (2002). A modified fuzzy c-means algorithm for bias field estimation and segmentation of MRI data. *IEEE transactions on medical imaging*, *21*(3), 193-199.

16. Zadeh, L. A. (1996). Fuzzy sets. In Fuzzy Sets, Fuzzy Logic, And Fuzzy Systems: Selected Papers by Lotfi A Zadeh (pp. 394-432).
17. Chen, S., & Zhang, D. (2004). Robust image segmentation using FCM with spatial constraints based on new kernel-induced distance measure. *IEEE Transactions on Systems, Man, and Cybernetics, Part B (Cybernetics)*, *34*(4), 1907-1916.
18. Szilagyi, L., Benyo, Z., Szilágyi, S. M., & Adam, H. S. (2003, September). MR brain image segmentation using an enhanced fuzzy c-means algorithm. In *Engineering in Medicine and Biology Society, 2003. Proceedings of the 25th Annual International Conference of the IEEE* (Vol. 1, pp. 724-726). IEEE.
19. Cai, W., Chen, S., & Zhang, D. (2007). Fast and robust fuzzy c-means clustering algorithms incorporating local information for image segmentation. *Pattern recognition*, *40*(3), 825-838.
20. Krinidis, S., & Chatzis, V. (2010). A robust fuzzy local information C-means clustering algorithm. *IEEE transactions on image processing*, *19*(5), 1328-1337.
21. Zaixin, Z., Lizhi, C., & Guangquan, C. (2013). Neighbourhood weighted fuzzy c-means clustering algorithm for image segmentation. *IET Image Processing*, 8(3), 150-161.
22. Harish, B. S., Kumar, S. A., Masulli, F., & Rovetta, S. (2017). Adaptive Initialization of Cluster Centers using Ant Colony Optimization: Application to Medical Images. In *ICPRAM* (pp. 591-598).
23. Chang, C. W., Ho, C. C., & Chen, J. H. (2012). ADHD classification by a texture analysis of anatomical brain MRI data. *Frontiers in systems neuroscience*, *6*, 66.

24. Lee, J. Y., Mun J. Y., Taheri, M., Son, S. H., & Shin, S. (2017, September). Vessel Segmentation Model using Automated Threshold Algorithm from Lower Leg MRI. *In Proceedings of the International Conference on Research in Adaptive and Convergent Systems* (pp. 120-125). ACM.
25. Smith, S. M. (2002). Fast robust automated brain extraction. *Human brain mapping*, *17*(3), 143-155.
26. Cox, R. W. (1996). AFNI: software for analysis and visualization of functional magnetic resonance neuroimages. *Computers and Biomedical research*, *29*(3), 162-173.
27. Ojala, T., Pietikäinen, M., & Harwood, D. (1996). A comparative study of texture measures with classification based on featured distributions. *Pattern recognition*, *29*(1), 51-59.
28. Ojala, T., Pietikainen, M., & Maenpaa, T. (2002). Multiresolution gray-scale and rotation invariant texture classification with local binary patterns. *IEEE Transactions on pattern analysis and machine intelligence*, *24*(7), 971-987.
29. Larroza, A., Bodí, V., & Moratal, D. (2016). Texture analysis in magnetic resonance imaging: Review and considerations for future applications. In *Assessment of Cellular and Organ Function and Dysfunction using Direct and Derived MRI Methodologies*. InTech.
30. Zhao, G., & Pietikainen, M. (2007). Dynamic texture recognition using local binary patterns with an application to facial expressions. *IEEE transactions on pattern analysis and machine intelligence*, *29*(6), 915-928.
31. BrainWeb: Simulated Brain Database(http://www.bic.mni.mcgill.ca/brainweb/)

32. Collins, D. L., Zijdenbos, A. P., Kollokian, V., Sled, J. G., Kabani, N. J., Holmes, C. J., & Evans, A. C. (1998). Design and construction of a realistic digital brain phantom. *IEEE transactions on medical imaging*, *17*(3), 463-468.
33. Cocosco, C. A., Kollokian, V., Kwan, R. K. S., Pike, G. B., & Evans, A. C. (1997). Brainweb: Online interface to a 3D MRI simulated brain database. In *NeuroImage*.
34. Aubert-Broche, B., Evans, A. C., & Collins, L. (2006). A new improved version of the realistic digital brain phantom. *NeuroImage*, *32*(1), 138-145.
35. Aubert-Broche, B., Griffin, M., Pike, G. B., Evans, A. C., & Collins, D. L. (2006). Twenty new digital brain phantoms for creation of validation image data bases. *IEEE transactions on medical imaging*, *25*(11), 1410-1416.
36. Yeghiazaryan, V., & Voiculescu, I. (2015). *An overview of current evaluation methods used in medical image segmentation*. Tech. Rep. CS-RR-15-08, Department of Computer Science, University of Oxford, Oxford, UK.
37. Dunn, J. C. (1973). A fuzzy relative of the ISODATA process and its use in detecting compact well-separated clusters.
38. Fuzzy C-Means Clustering for Iris Data. (n.d.). Retrieved from https://www.mathworks.com/help/fuzzy/examples/fuzzy-c-means-clustering-for-iris-data.html